

# Solvent Effect on Rb<sup>+</sup> to K<sup>+</sup> Ion Mutation: Monte Carlo Simulation Study

Hag-Sung Kim

Department of Industrial Chemistry, Ulsan College, Ulsan 680-749, Korea

Received January 19, 2000

The solvent effects on the relative free energies of solvation and the difference in partition coefficients ( $\log P$ ) for Rb<sup>+</sup> to K<sup>+</sup> mutation in several solvents have been investigated using Monte Carlo simulation (MCS) of statistical perturbation theory (SPT). In comparing the relative free energies for interconversion of one ion pair, Rb<sup>+</sup> to K<sup>+</sup>, in H<sub>2</sub>O (TIP4P) in this study with the relative free energies of the computer simulations and the experimental, we found that the figure in this study is  $-5.00 \pm 0.11$  kcal/mol and those of the computer simulations are  $-5.40 \pm 1.9$ ,  $-5.5$ , and  $-5.4$  kcal/mol. The experimental is  $-5.1$  kcal/mol. There is good agreement among various studies, taking into account both methods used to obtain the hydration free energies and standard deviations. There is also good agreement between the calculated structural properties of this study and the simulations, ab initio and the experimental results. We have explained the deviation of the relationship between the free energy difference and the Onsager dielectric function of solvents by the electron pair donor properties of the solvents. For the Rb<sup>+</sup> and K<sup>+</sup> ion pair, the Onsager dielectric function of solvents (or solvent permittivity), donor number of solvent and the differences in solvation dominate the differences in the relative free energies of solvation and partition coefficients.

## Introduction

The study of metal ions in solution is one of the most active areas in solution chemistry due to the large number of physicochemical and biochemical properties directly controlled or indirectly conditioned by ionic effects in many fields of chemistry, biochemistry, and chemical engineering.<sup>1-5</sup> Due to the large number of particles forming these systems and the variety of different interactions established, computer simulations represent a particularly adequate theoretical tool for understanding and predicting the physicochemical properties of those solutions at the microscopic level.<sup>6-8</sup> Understanding the phenomena related to the solvation of ionic species has been an important quest in chemical physics, and of course in many related field, where this phenomenon has a relevant role. Many interesting problems in biomolecular and biomimetic chemistry involve interaction with metal (or other) ions in one way or other.

Cyclacenes and collarenes<sup>9</sup> are known to behave as ionophores and receptors. These molecules interact with cations by the cation- $\pi$  interaction<sup>10a,b</sup> discovered by Doughterty and his coworkers.<sup>10</sup> The differences in cationic affinity for cyclacenes and collarenes are interesting issues. Cyclodepsipeptides are often present in biological systems, many of which are complexing agents for alkali and alkaline earth metal cations.<sup>11</sup> The differences in cationic affinity for amide carbonyl groups or ester carbonyl groups in cyclodepsipeptides are also interesting issues. Therefore, it is important to investigate their structure as well as binding energetics with cations. And complexing agents like crown ethers and cryptands are also known to effect a dramatic change in the interaction of cations with their counterions.<sup>12</sup>

To understand those questions and phenomena, we need information on cation stability ordering in solution. This could be obtained from the relative free energies of ion mutation in solution. Several statistical mechanical procedures have evolved for computing free energy differences. Two particularly promising approaches are umbrella sampling<sup>13-17</sup> and a perturbation procedure<sup>18-20</sup> in which one ion is mutated into the other. The ability to accurately calculate solvation free energies of molecules using perturbation procedure is one of the important and recent developments in computational chemistry.<sup>20</sup> The distribution of an ion binding organic solute between polar or less polar and non-polar media is an important parameter for structure-activity analyses in pharmacological research.<sup>21-23</sup> Many procedures have been devised to estimate the logarithm of the partition coefficient ( $\log P$ ) for a solute between water and solvents.<sup>21-25</sup>

It is known that solvent effects often play an important role in determining equilibrium constants, transition states and rates of reactions,  $\pi$ -facial selectivity, conformations, and other quantities of chemical, chemical physics and biochemical interest.

But, few studies of solvent effects on both the relative free energies of solvation and the difference in partition coefficients ( $\log P$ ) for alkali metal ions are available.

In this study, we have studied solvent effect on interconversion of one alkali metal ion pair, Rb<sup>+</sup> to K<sup>+</sup>, using Monte Carlo simulations with statistical perturbation theory (SPT). The following solvents were selected: H<sub>2</sub>O (TIP3P, TIP4P models), CHCl<sub>3</sub>, CH<sub>3</sub>CN, THF, CH<sub>3</sub>OH, CCl<sub>4</sub>, CH<sub>3</sub>Cl<sub>2</sub>, MeOMe, and C<sub>2</sub>H<sub>8</sub>. They were chosen because they have the variety of the solvent properties and the availability of potential function parameters.<sup>26</sup> The fundamental and theoretical approach to computing solvent effect on differences in partition coefficients as well as the relative free energies is, for the first time, explored based on fluid simulations at the

\*Corresponding author. Tel: +82-522-279-3176, Fax: +82-522-277-1538, E-mail: hskim@mail.ulsan-c.ac.kr

atomic level for those ions in this study. This study provides some insight into solvent effect on not only variations of the  $\Delta G_1$  and  $\Delta G_2$  components in Eq. (5) and helps assess the viability of this solvent effect approach to estimating  $\Delta \log P$ . This study also provides additional interests of the solvent effect on equilibrium constants, transition states, rates of the organic reaction,  $\pi$ -facial selectivity,<sup>10c</sup> conformations, and the other quantities of chemical, biochemical interest and chemical-physics.

### Computational Procedure

The procedure used here is similar to that employed to study interconversion of organic solutes and ions mutation.<sup>27-28</sup> The modeled systems consisted of the ion plus 260 solvent molecules in a cubic cell with periodic boundary conditions. First, the Monte Carlo simulations are described, including a summary of the method for computing the relative free energy changes and then a brief discussion of the potential functions is given.

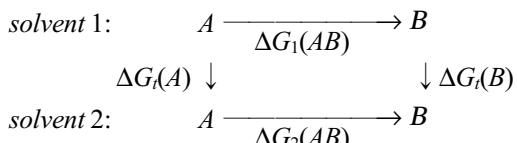
**Monte Carlo Simulations.** Monte Carlo simulations were carried out in the isothermal-isobaric ensemble at 25°C and 1atm for systems typically consisting of the ion plus 260 solvent molecules in a cubic cell with periodic boundary conditions. The free energy changes,  $\Delta G_1$  and  $\Delta G_2$ , were obtained via a series of 5 separate simulations with SPT.<sup>20,29</sup> In Monte Carlo simulations with SPT, we used doublewide sampling.<sup>27</sup>

The perturbation approach is based on Eq. (1),<sup>29</sup>

$$G_i - G_j = -k_B T \ln \langle \exp(-(E_i - E_j)/k_B T) \rangle_j \quad (1)$$

in which  $k_B$  is Boltzmann constant,  $T$  is the temperature,  $E$  is the total potential energy for the full system,  $i$  and  $j$ . The free energy difference between a reference system,  $j$ , and a perturbed system,  $i$ , is given as a function of the average energy difference between the two systems.<sup>29</sup> The notation  $\langle \dots \rangle_j$  implies that the configurational sampling is based on the reference system.

If one considers the thermodynamic cycle below for two ions, A and B, in two solvents,  $\log P$  for the ions is defined in Eq. (2) and (3) in terms of the free energies of transfer.



$$\Delta G_1(A) = -2.3RT \log P_A \quad (2)$$

$$\Delta G_2(B) = -2.3RT \log P_B \quad (3)$$

From the cycle, Eq. (4) is obtained, which yields Eq. (5).

$$\Delta G_t(B) - \Delta G_t(A) = \Delta G_2(AB) - \Delta G_1(AB) \quad (4)$$

$\Delta \log P = \log P_B - \log P_A = (\Delta G_2(AB) - \Delta G_1(AB))/2.3RT$  (5)  
The last expression associates the difference in  $\log P$ 's with the difference in free energies for mutating A to B in the two solvents.

$\Delta G_1$  and  $\Delta G_2$  are available from Monte Carlo simulations

in which A is mutated to B in the solvents. Computations of this type have been used in a range of applications, including some preliminary results for relative partition coefficients.<sup>30</sup> It may be noted that absolute  $\log P$ 's could also be computed by directly calculating the free energy of transfer. This would require taking the difference in absolute free energies of solvation for the ion, which could be obtained from simulations in which the ion is made to vanish in the two solvents.<sup>31,32</sup>

In this study, each simulation entailed an equilibration period for  $1 \times 10^6$  configurations starting from equilibrated boxes of solvent, followed by averaging for  $2 \times 10^6$  configurations. Little drift in the averages was found during the last  $1 \times 10^6$  configurations.<sup>27</sup> Metropolis and preferential sampling were employed, and the ranges for attempted translations and rotations of the solute and solvent molecules were adjusted to give an approximately 45% acceptance rate for new configurations.<sup>27</sup>

**Intermolecular Potential Functions.** The solvent-solvent and ion-solvent interactions were described by potential function in the standard Lennard-Jones plus Coulomb format (Eq. 6).

$$\Delta E = \sum_i \sum_j (q_i q_j e^2 / r_{ij} + A_{ij} / r_{ij}^{12} - C_{ij} / r_{ij}^{16}) \quad (6)$$

The ion and molecules are represented by interaction sites located on nuclei that have associated charge,  $q_i$  and Lennard-Jones parameter  $\sigma_i$  and  $\epsilon_i$ . Standard combining rules are used such that  $A_{ij} = (A_{ii}A_{jj})^{1/2}$  and  $C_{ij} = (C_{ii}C_{jj})^{1/2}$ . Furthermore, the  $A$  and  $C$  parameters may be expressed as  $A_{ij} = 4\epsilon_i \sigma_i^{12}$  and  $C_{ij} = 4\epsilon_i \sigma_i^6$ , where  $\sigma$  and  $\epsilon$  are the Lennard-Jones radius and energy terms and  $i$  and  $j$  indices span all of the solvents and water sites.

The OPLS (optimized potential for liquid simulation) potential parameter for the ion and solvents are used and those are based on a united-atom model.<sup>26,33</sup> However, the TIP4P and TIP3P model has been used for water.<sup>34</sup>

The charges and Lennard-Jones parameters have been selected to yield correct thermodynamic and structural results for pure liquids.<sup>34</sup> They are listed in Table 1. The results were obtained from Monte Carlo simulations using well-established procedures.<sup>29-32</sup> In all the calculations, the bond lengths and bond angles have been kept fixed. The intermolecular interactions, *i.e.* long-range forces, were spherically truncated at 8.5, 10, 12.0 Å, depending on box-sizes of the solvents and the reaction field method was used.<sup>26</sup>

### Results and Discussion

**Relative free energies.** To explore solvent effect on the differences in partition coefficients as well as the relative free energies for interconversion of one ion pair, Rb<sup>+</sup> to K<sup>+</sup>, obtained from a Monte Carlo statistical simulation study, we computed the relative free energy of H<sub>2</sub>O (TIP4P) for comparison with the experimental and computer simulations of H<sub>2</sub>O. We have also computed those in the other solvents.

The relative free energies for interconversion of one ion pair, Rb<sup>+</sup> to K<sup>+</sup>, from the present calculations along with the

**Table 1.** OPLS potential parameters for several solvents

Solvent	site	q, e	$\sigma \text{ \AA}$	$\epsilon \text{ kcal/mol}$
H <sub>2</sub> O(TIP4P)	OW	0.0000	3.1536	0.1550
	HW	0.5200	0.0000	0.0000
	HW	0.5200	0.0000	0.0000
	M <sup>a</sup>	-1.0400	0.0000	0.0000
H <sub>2</sub> O(TIP3P)	OW	-0.8340	3.1506	0.1521
	HW	0.4170	0.0000	0.0000
	HW	0.4170	0.0000	0.0000
	C	0.2800	3.6500	0.1500
CH <sub>3</sub> CN	N	-0.4300	3.2000	0.1700
	CH <sub>3</sub>	0.1500	3.7750	0.2070
	O	-0.7000	3.0700	0.1700
CH <sub>3</sub> OH	H	0.4350	0.0000	0.0000
	CH <sub>3</sub>	0.2650	3.7750	0.2070
	CH <sub>2</sub>	0.5000	3.8000	0.1180
CH <sub>2</sub> Cl <sub>2</sub>	Cl	-0.2500	3.4000	0.3000
	Cl	-0.2500	3.4000	0.3000
	O	-0.5000	3.0000	0.1700
THF	CH <sub>2</sub>	0.2500	3.8000	0.1180
	CH <sub>2</sub>	0.0000	3.9050	0.1180
	CH <sub>2</sub>	0.2500	3.8000	0.1180
	CH <sub>2</sub>	0.0000	3.9050	0.1180
	O	-0.5000	3.0000	0.1700
MeOMe	CH <sub>3</sub>	0.2500	3.8000	0.1700
	CH <sub>3</sub>	0.2500	3.8000	0.1700
	O	-0.5000	3.0000	0.1700
CHCl <sub>3</sub>	CH	0.4200	3.8000	0.0800
	Cl	-0.1400	3.4700	0.3000
	Cl	-0.1400	3.4700	0.3000
	Cl	-0.1400	3.4700	0.3000
CCl <sub>4</sub>	C	0.2480	3.8000	0.0500
	Cl	-0.0620	3.4700	0.2660
	Cl	-0.0620	3.4700	0.2660
	Cl	-0.0620	3.4700	0.2660
	Cl	-0.0620	3.4700	0.2660
C <sub>3</sub> H <sub>8</sub>	CH <sub>2</sub>	0.0000	3.9050	0.1180
	CH <sub>3</sub>	0.0000	3.9050	0.1750
	CH <sub>3</sub>	0.0000	3.9050	0.1750

<sup>a</sup>M is a point on the bisector of HOH angle, 0.15 Å from the oxygen toward the hydrogens.

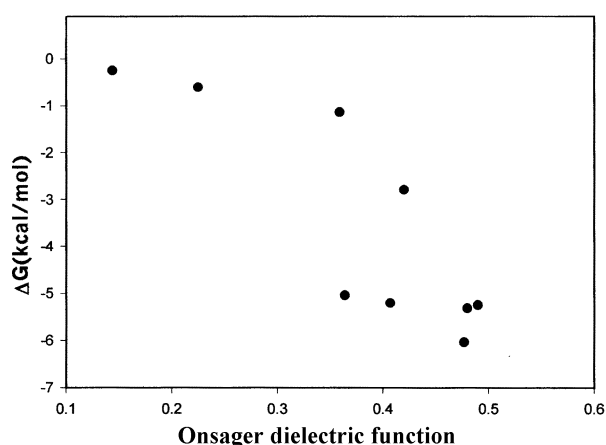
computer simulations are listed in Table 2. The relative free energies of solvation versus the Onsager dielectric function of solvent (permittivity) are plotted in Figure 1. The computed ordering of the free energies of solvation in several solvents is C<sub>3</sub>H<sub>8</sub> > CCl<sub>4</sub> > CHCl<sub>3</sub> > CH<sub>2</sub>Cl<sub>2</sub> > MeOMe > THF > H<sub>2</sub>O(TIP4P) > CH<sub>3</sub>CN > H<sub>2</sub>O(TIP3P) > CH<sub>3</sub>OH. This comes about by the change in solvation free energies for A going to B which is more favorable in CH<sub>3</sub>OH than in the polar and less polar or non-polar solvents ( $\Delta G_1 < \Delta G_2$ ).

As shown in Figure 1, the relative free energies of solvation vs. the Onsager dielectric function of solvent have two groups. One decreases with increasing Onsager dielectric function of solvents. This trend of the relative free energies of solvation could be explained by the differences in solvation. The other trend is that of CH<sub>3</sub>OH, CH<sub>3</sub>CN, THF and MeOMe. The relative free energies of solvation Rb<sup>+</sup>/K<sup>+</sup> pair in CH<sub>3</sub>OH, CH<sub>3</sub>CN, THF and MeOMe could be explained

**Table 2.** Relative Gibbs Free Energies (kcal/mol) of solvation in several solvents and permittivity( $\epsilon$ ) and Onsager dielectric function ( $\epsilon - 1/2\epsilon + 1$ )<sup>d</sup> of solvents

Solvent	$\Delta G(\text{Rb}^+ \rightarrow \text{K}^+)$	$\epsilon^e$	$\epsilon - 1/2\epsilon + 1$
H <sub>2</sub> O(TIP3P)	-5.57 ± 0.06	78.3	0.490
H <sub>2</sub> O(TIP4P)	-5.00 ± 0.11	78.3	0.490
H <sub>2</sub> O(rigid SPC) <sup>f</sup>	-5.40 ± 1.9	78.3	0.490
H <sub>2</sub> O(LD-CS2) <sup>b</sup>	-5.5	78.3	0.490
H <sub>2</sub> O(SPC) <sup>c</sup>	-5.4 ± 1.9	78.3	0.490
Experiment <sup>d</sup>	-5.1	78.3	0.490
CH <sub>3</sub> CN	-5.06 ± 0.07	36.64	0.480
CH <sub>3</sub> OH	-5.83 ± 0.08	32.66	0.477
CH <sub>2</sub> Cl <sub>2</sub>	-2.70 ± 0.05	8.93	0.420
THF	-4.99 ± 0.11	7.58	0.407
MeOMe	-4.86 ± 0.06	5.02	0.364
CHCl <sub>3</sub>	-1.12 ± 0.03	4.81	0.359
CCl <sub>4</sub>	-0.62 ± 0.03	2.23	0.225
C <sub>3</sub> H <sub>8</sub>	-0.28 ± 0.02	1.16 <sup>f</sup>	0.144

<sup>a</sup>ref. 38. <sup>b</sup>ref. 39. <sup>c</sup>ref. 40. <sup>d</sup>ref. 1. <sup>e</sup>Gaussian98 Users Reference 1998, p162. <sup>f</sup>273K data from "Handbook of Chem. & Phys." 71<sup>st</sup> Ed. C.R.C. Press 1990.

**Figure 1.** Plot of relative Gibbs free energy of solvation vs. Onsager dielectric function of solvents at 298 K and 1 atm.

by the fact that the strong ion-solvent interactions exist in CH<sub>3</sub>OH, CH<sub>3</sub>CN, THF and MeOMe solutions even though the Onsager dielectric function of CH<sub>3</sub>OH, CH<sub>3</sub>CN, THF and MeOMe are small. The strong ion-solvent interactions in CH<sub>3</sub>OH, CH<sub>3</sub>CN, THF and MeOMe solutions are due to the electron pair donor properties of the solvents to ion, i.e., donor number (DN) of CH<sub>3</sub>OH, CH<sub>3</sub>CN, THF and MeOMe established by Gutmann.<sup>35</sup>

In the absence of strong hydrogen bonding, the molecule or ion with the larger dipole moment could be expected to be more favorably solvated.<sup>36</sup> The Rb<sup>+</sup>/K<sup>+</sup> pair in C<sub>3</sub>H<sub>8</sub> provides a striking exception that points out the importance of local electrostatic interactions or higher multipole moments.<sup>37</sup> The computed difference in free energies of solvation for ions in C<sub>3</sub>H<sub>8</sub> is comparatively small.

Clearly, the replacement of the stronger ion-solvent interactions with the weaker ion-dipole interactions is responsible for the decreasing effect.

Comparing the relative free energies for interconversion of

the solute ions,  $\text{Rb}^+$  to  $\text{K}^+$ , in  $\text{H}_2\text{O}$  (TIP3P) in this study with those in refs. 38, 39, 40 and 1. That of  $\text{H}_2\text{O}$  (TIP4P) is  $-5.00 \pm 0.11$  kcal/mol in this study, that in ref. 38 is  $-5.40 \pm 1.9$  kcal/mol, obtained from hydration free energies of  $\text{Rb}^+$  ( $-75.5 \pm 0.9$  kcal/mol) and  $\text{K}^+$  ( $-80.9 \pm 1.0$  kcal/mol), that of experiment in ref. 1 is  $-5.1$  kcal/mol, that in ref. 39 is  $-38.8$  kcal/mol, obtained from hydration free energies  $\text{Rb}^+$  ( $-75.4$  kcal/mol) and  $\text{K}^+$  ( $-80.9$  kcal/mol) and that in ref. 40 is  $-5.40$  kcal/mol obtained, from hydration free energies of and  $\text{Rb}^+$  ( $-75.5 \pm 0.9$  kcal/mol) and  $\text{K}^+$  ( $-80.9 \pm 1.0$  kcal/mol), respectively. There is good agreement among several studies if we consider both methods used to obtain the hydration free energies and standard deviations. From this comparison, the computed data for the other solvents are expected to be reliable. The relative free energies for interconversion of one ion pair,  $\text{Rb}^+$  to  $\text{K}^+$ , in  $\text{H}_2\text{O}$  (TIP3P) are smaller than that of  $\text{H}_2\text{O}$  (TIP4P). This difference of solvation could be explained by the difference in polarity between two-water models. The trend of binding energies of cyclodepsipeptides and [n] col-larenes with those ions obtained by ab initio are coincident with our results for the relative free energies of hydration.<sup>9,11</sup>

**Partition coefficients.** The calculated logarithms of solvents/ water [ $\text{H}_2\text{O}$  (TIP3P)] partition coefficients are listed in Table 3. If contributions from internal degrees of freedom are ignored,  $\Delta G_1$  and  $\Delta G_2$  in Eq. 5 are just the difference between free energies of solvation for A and B. For example, if solvent 1 is  $\text{CH}_3\text{OH}$  and solvent 2 is the polar and less polar or non-polar solvent, larger values of  $\log P$  imply that the change from  $\text{Rb}^+$  to  $\text{K}^+$  results in greater affinity for  $\text{CH}_3\text{OH}$  over the polar and less polar or non-polar solvent. And larger values of  $\Delta \log P$  indicate that the change from  $\text{Rb}^+$  to  $\text{K}^+$  results in increased affinity for the  $\text{CH}_3\text{OH}$  over the other solvents. We could not compare the data from this study with previously published results because there were no studies for logarithms of solvents/ $\text{CH}_3\text{OH}$  partition coefficients for interconversion of one ion pair,  $\text{Rb}^+/\text{K}^+$ .

It is necessary to note that the sign and magnitude of the calculated  $\Delta \log P$ 's closely parallel the relative free energies of solvation. This reflects the limited variation in the free energies of solvation in  $\text{C}_3\text{H}_8$  relative to the other solvents and emphasizes the dominance of the free energies of solvation in determining, the partitioning behavior in other solvents versus  $\text{C}_3\text{H}_8$ .

**Structural properties.** The solvation structure can be

**Table 3.** Differences in the logarithms of solvents/ $\text{CH}_3\text{OH}$  partition coefficients

Solvent	$\log P_B - \log P_A$
$\text{H}_2\text{O}$ (TIP3P)	0.19
$\text{H}_2\text{O}$ (TIP4P)	0.61
$\text{CH}_3\text{CN}$	0.56
$\text{CH}_2\text{Cl}_2$	2.30
THF	0.62
$\text{MeOMe}$	0.71
$\text{CHCl}_3$	3.46
$\text{CCl}_4$	3.83
$\text{C}_3\text{H}_8$	4.08

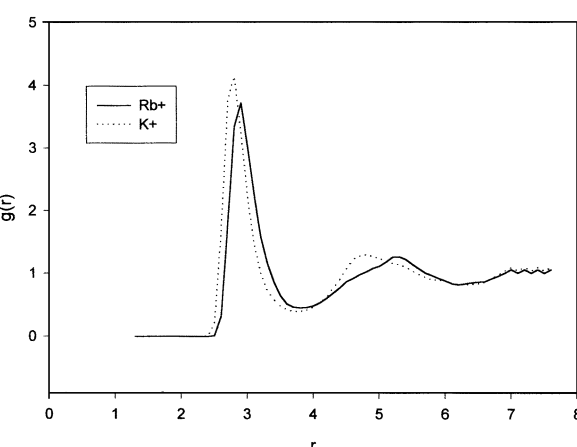


**Figure 2.** Computed radial distribution function between O and  $\text{Rb}^+$  ( $\text{H}_2\text{O}$  (TIP4P)) and ion converted from  $\text{Rb}^+$  to  $\text{K}^+$ . Distances are in angstroms throughout.

characterized through radial distribution functions (rdfs),  $g_{ab}(r)$ , which give the probability of finding an atom of type *b* at a distance *r* from an atom of type *a*. The calculated rdbs of atom- $\text{Rb}^+/\text{K}^+$  ion are shown in Figure 2 to Figure 6 and have been sorted into four patterns, according to the solvents. The positions of the first maximum in ion-(O, N, Cl and  $\text{CH}_2$ ) in solvents obtained from rdbs are listed in Table 4(a). They decrease when  $\text{Rb}^+$  ion transforms to  $\text{K}^+$  ion in all solvents. The numbers of solvent molecules in the first coordination shell of  $\text{Rb}^+/\text{K}^+$  ions can be evaluated by integrating ion-(O, N, Cl and  $\text{CH}_2$ ) in solvents rdbs to their first minimum. See Table 4(a). The number of solvent molecules in the first coordination shell of  $\text{Rb}^+/\text{K}^+$  ions also decreases when  $\text{Rb}^+$  ion transforms to  $\text{K}^+$  ion in all solvents except for  $\text{CHCl}_3$ .

The rdbs of atom- $\text{Rb}^+/\text{K}^+$  ion in solvents that have O atom display two well-defined peaks, whereas the  $\text{Rb}^+$  ion transform to the  $\text{K}^+$  ion. In the first rdf's pattern shown in Figure 2 to Figure 3, the atom (O) in solvents- $\text{Rb}^+/\text{K}^+$  ion hydrogen bonding is reflected in the high, first peak in rdbs. But as  $\lambda$  increases, the maximum peak positions of O- $\text{Rb}^+/\text{K}^+$  ion rdbs move to the smaller *r* value as shown in Figure 2 to Figure 3, and the intensity of the maximum peak of O- $\text{Rb}^+/\text{K}^+$  ion rdbs increases. This means that the O-ion bonding features become stronger as  $\lambda$  increases and  $\text{Rb}^+$  ion smoothly transforms to  $\text{K}^+$  ion.

Experimental data of the ion-solvent structure in  $\text{Rb}^+$  and  $\text{K}^+$  ions aqueous solutions are essentially limited to the first shell. In Table 4(b) and (c), the positions of the first maximum in ion-oxygen rdf's obtained from this study are compared with various simulations, ab initio and the experimental results.<sup>38-45</sup> There is good agreement between our results and the simulations. The results of this study are uniformly good. Interestingly, the optimized bond lengths in small ion-molecule clusters using function from ab initio calculations agree well with the aqueous  $\text{K}^+$  solution.<sup>44</sup> Rao and Berne have noted that local solvation structures in aqueous ionic solutions are similar to those in relatively small clusters.<sup>46</sup>

The calculated coordination numbers for ions in aqueous solutions are also compared with the computer simulations

**Table 4.** Structural results for the first shell(a) Structural properties of Rb<sup>+</sup>/K<sup>+</sup> ion in several solvents

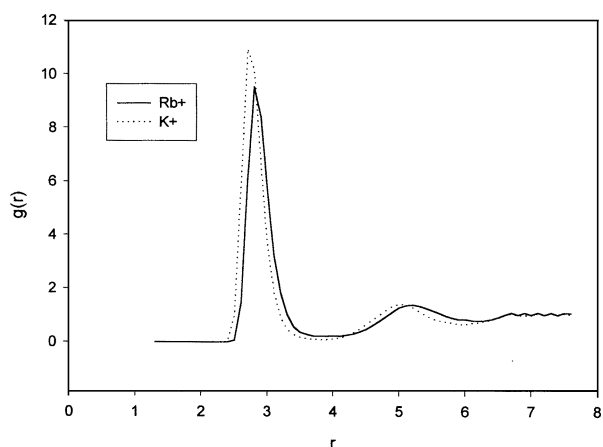
Solvent	Rb <sup>+</sup> ion		K <sup>+</sup> ion	
	R <sub>i-o</sub> (Å)	Coordination Number	R <sub>i-o</sub> (Å)	Coordination Number
H <sub>2</sub> O(TIP3P)	2.8	7.0	2.7	6.3
H <sub>2</sub> O(TIP4P)	2.9	7.6	2.8	7.4
CH <sub>3</sub> OH	2.8	6.0	2.7	6.0
THF	2.9	7.1	2.8	7.0
MeOMe	2.9	6.5	2.8	6.3
R <sub>i-N</sub> (Å)				
Coordination Number		Coordination Number		
CH <sub>3</sub> CN	2.9	7.5	2.8	7.4
(R <sub>i-Cl</sub> ) (Å)		Coordination Number		
CH <sub>2</sub> Cl <sub>2</sub>	3.2	4.5	3.1	4.0
CHCl <sub>3</sub>	3.5	2.4	3.4	2.7
CCl <sub>4</sub>	5.1	4.8	3.7	-
R <sub>i-CH<sub>2</sub></sub> (Å)		Coordination Number		
C <sub>3</sub> H <sub>8</sub>	5.0	5.0	4.8	4.1

(b) Structural properties of Rb<sup>+</sup> and K<sup>+</sup> ions in water (TIP4P)

	Rb <sup>+</sup>	K <sup>+</sup> ion
Ion-Oxygen Distance(Å)		
This work	2.90	2.80
Åqvist <sup>a</sup>	2.89	2.75
Heinzinger <sup>b</sup>	-	2.80
Lee and Rasaish <sup>c</sup>	2.90	2.79
Exp. <sup>d</sup>	2.88	2.80
Kollman <sup>e</sup>	-	2.7
Kim <sup>f</sup>	-	2.83
Chang and Dang <sup>g</sup>	-	2.75
Ion-Hydrogen Distance(Å)		
This work	3.40	3.4
Heinzinger <sup>b</sup>	-	3.52
Dang <sup>g</sup>	-	3.35
Coordination Number		
This work	7.6	7.4
Lee and Rasaish <sup>c</sup>	7.8	7.2
Exp. <sup>d</sup>	-	6.0, 7.0
Kollman <sup>e</sup>	-	4-5
Kim <sup>f</sup>	-	6.0
Chang and Dang <sup>g</sup>	-	7.3

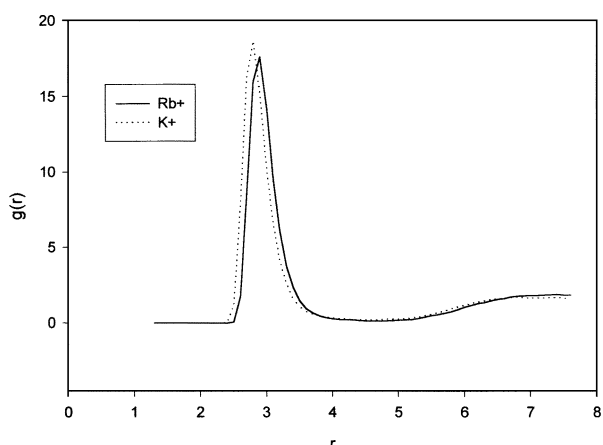
<sup>a</sup>ref. 38. <sup>b</sup>ref. 41. <sup>c</sup>ref. 42. <sup>d</sup>ref. 1. <sup>e</sup>ref. 43. <sup>f</sup>ref. 44. <sup>g</sup>ref. 45.

and the experimental results in Table 4(b) and (c). Both the calculated and the experimental results are sensitive to the definition of coordination number. A wide range of experimental hydration numbers is available from mobility measurements.<sup>47</sup> These values correspond to the number of solvent molecules that have undergone some constant critical change due to the ion, a change that is susceptible to measurement by a particular experimental technique. Such hydration numbers are often quite different from coordination numbers based on a structural definition, like those from

**Figure 3.** Computed radial distribution function between O atom of CH<sub>3</sub>OH and ion converted from Rb<sup>+</sup> to K<sup>+</sup>.diffraction experiments.<sup>48</sup>

Mezei and Beveridge obtained their values by integrating the ion-center of mass of water rdf's up to the minimum of the first peaks.<sup>49</sup> These values will not be significantly different if they are based on ion-oxygen rdf's. This is a straightforward definition and this has been adopted for all the calculated values for those ions. For the present results, the coordination number is reported on the basis of integration to the minimum after the first peak in the ion-oxygen. As shown in Table 4 (b) and (c), the calculated coordination numbers from the ion-oxygen rdf's compare favorably with the various simulations, *ab initio* and experimental results taking into account the problems in the definition. Based on this comparison, the computed structural properties data in the other solvents are expected to be reliable

The second pattern of the rdf's of the O-atom in solvents-Rb<sup>+</sup>/K<sup>+</sup> ion displays one well-defined peak, while the Rb<sup>+</sup> ion is transformed to the K<sup>+</sup> ion as shown in Figure 4. But the O atom in solvents- Rb<sup>+</sup>/K<sup>+</sup> ion bonding is also reflected in the high, narrow first peak in the rdf's. As  $\lambda$  increases, the maximum peak positions of the O atom in solvents- Rb<sup>+</sup>/K<sup>+</sup> ion rdf's also move to the smaller r value as shown in the first pattern rdf's. The intensity of the maximum peak of the O

**Figure 4.** Computed radial distribution function between O atom of THF and ion converted from Rb<sup>+</sup> to K<sup>+</sup>.

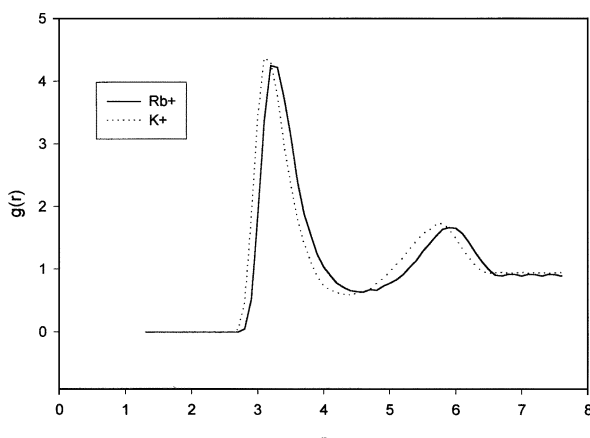


**Figure 5.** Computed radial distribution function between Cl of  $\text{CH}_2\text{Cl}_2$  and ion converted from  $\text{Rb}^+$  to  $\text{K}^+$ .

atom in solvents-  $\text{Rb}^+/\text{K}^+$  ion rdf's has also increased. This also means that the O-ion bonding features become stronger as  $\lambda$  increases and the  $\text{Rb}^+$  ion smoothly transforms to the  $\text{K}^+$  ion.

The third pattern of the rdf's of the Cl atom in solvents-  $\text{Rb}^+/\text{K}^+$  ion displays two broadly defined peaks, whereas the  $\text{Rb}^+$  ion transform to the  $\text{K}^+$  ion as shown in Figure 5. But the Cl atom in solvents-  $\text{Rb}^+/\text{K}^+$  ion interactions is reflected more in the broader first peak in the rdf's than in the first peak of the previous pattern rdf's. As  $\lambda$  increases, the maximum peak positions of the Cl atom in solvents-  $\text{Rb}^+/\text{K}^+$  ion rdf's also move to the smaller  $r$  value as shown in the first pattern rdf's and the intensity of the maximum peak of the Cl atom in solvents-  $\text{Rb}^+/\text{K}^+$  ion rdf's have also increased. This means that the solvent-ion interactions become stronger as  $\lambda$  increases, and the  $\text{Rb}^+$  ion smoothly transforms to the  $\text{K}^+$  ion.

The last pattern of the rdf's is shown in Figure 6. In Figure 6, the rdf's of the Cl in the solvents-  $\text{Rb}^+/\text{K}^+$  ion display one broadly defined peak, and the  $\text{Rb}^+$  ion transforms to the  $\text{K}^+$  ion. The Cl in the solvents-  $\text{Rb}^+/\text{K}^+$  ion weak interactions is reflected in the broader peak in the rdf's than in the first peak of the previous pattern rdf's. As  $\lambda$  increases, the maximum peak positions of the Cl in solvents-  $\text{Rb}^+/\text{K}^+$  ion rdf's also move to the smaller  $r$  value, as shown in the first pattern rdf's and the intensity of the maximum peak of the Cl in solvents-  $\text{Rb}^+/\text{K}^+$  ion rdf's have also increased. This also means that the solvent-ion interactions are becoming stronger as  $\lambda$  increases and the  $\text{Rb}^+$  ion smoothly transforms to the  $\text{K}^+$  ion.

### Conclusion

From this study we conclude that Monte Carlo simulations using SPT is a good approach to estimating changes in  $\log P$  that accompany ion transformation, *i.e.*  $\text{Rb}^+$  to  $\text{K}^+$  ion mutation. We have compared the relative free energies for interconversion of one ion pair,  $\text{Rb}^+$  to  $\text{K}^+$ , in  $\text{H}_2\text{O}$  (TIP4P) in this study with the published works. That of  $\text{H}_2\text{O}$  (TIP4P) is  $-5.00 \pm 0.11$  kcal/mol in this study, those of the published works are  $-5.40 \pm 1.9$  kcal/mol,  $-5.1$  kcal/mol,  $-38.8$  kcal/mol and  $-5.40$  kcal/mol, respectively. There is good agreement among several studies if we consider both methods used to obtain the hydration free energies and the standard deviations. We have also explained the deviation of the relationship between the free energy difference and Onsager dielectric function by the electron pair donor properties of the solvent. The calculated radial distribution functions (rdf) of atom- $\text{K}^+/\text{Na}^+$  ion have been sorted into four patterns according to the solvents. There is also good agreement between the calculated structural properties in this study and the computer simulations, ab initio and experimental results. For the present ion pairs, the Onsager dielectric function (or solvent permittivity), donor number of the solvent and the differences in solvation dominate the differences in the relative free energies of solvation and partition coefficients.

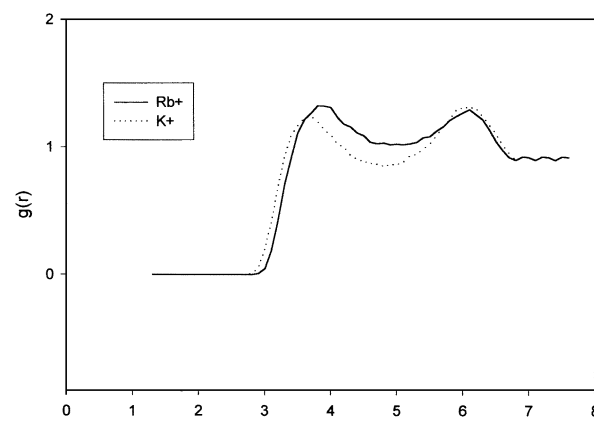


**Figure 6.** Computed radial distribution function between Cl of  $\text{CCl}_4$  and ion converted from  $\text{Rb}^+$  to  $\text{K}^+$ .

mol and  $-5.40$  kcal/mol, respectively. There is good agreement among several studies if we consider both methods used to obtain the hydration free energies and the standard deviations. We have also explained the deviation of the relationship between the free energy difference and Onsager dielectric function by the electron pair donor properties of the solvent. The calculated radial distribution functions (rdf) of atom- $\text{K}^+/\text{Na}^+$  ion have been sorted into four patterns according to the solvents. There is also good agreement between the calculated structural properties in this study and the computer simulations, ab initio and experimental results. For the present ion pairs, the Onsager dielectric function (or solvent permittivity), donor number of the solvent and the differences in solvation dominate the differences in the relative free energies of solvation and partition coefficients.

The results, in this study, obtained from the Monte Carlo simulations with SPT appear to be a promising approach to providing estimates of the effects of solvent changes on partitioning behavior of ion pairs between polar solvent and the less polar or non-polar solvents. The results in this study also appear useful in providing the association properties of ionophores and cyclodepsipeptides with alkaline metals.

**Acknowledgment.** This work was supported in part by 2000 Ulsan College Fund.

### References

1. (a) Burgess, J. *Metal Ions in Solution*; Halsted Press: 1978; Chapter 5, (b) Ohtaki, H.; Radnai, T. *Chem. Rev.* **1993**, *93*, 1157.
2. Conway, B. E. *Ionic Hydration in Chemistry and Biophysics. Studies in Physical and Theoretical Chemistry*; Elsevier: Amsterdam, 1981; Vol. 12.
3. Marcus, Y. *Ion Solvation*; Wiley-Interscience: New York, 1985.
4. Bathel, J. M.; Krienke, H.; Kunz, W. *Physical Chemistry of Electrolyte Solutions*; Steinkopff: Darmstadt, 1998.
5. Warshel, A. *Computer Modeling of Chemical Reactions in Enzymes and Solutions*; John Wiley: New York, 1991.
6. Clementi, E. *Modern Techniques in Computational Chemistry*; Escom: Leiden, 1990; Chapter 1.

7. Allen, M. P.; Tidelsley, D. J. *Computer Simulation of Liquids*; Oxford University Press: Oxford, 1987.
8. Simkin, B. Y.; Sheikhet, I. I. *Quantum Chemical and Statistical Theory of Solution: A Comprehensive Approach*; Ellis Horwood: London, 1995.
9. Choi, H. S.; Suh, S. B.; Cho, S. J.; Kim, K. S. *Proc. Natl. Acad. Sci. USA* **1998**, *95*, 12094.
10. (a) Kim, K. S.; Lee, J. Y.; Lee, S. J.; Ha, H-K.; Kim, D. H. *J. Am. Chem. Soc.* **1994**, *116*, 7399. (b) Lee, J. Y.; Lee, S. J.; Choi, H. S.; Cho, S. J.; Ha, H-K.; Kim, K. S. *Chem. Phys. Lett.* **1995**, *232*, 67. (c) Hong, B. H.; Lee, J. Y.; Cho, S. J.; Kim, K. S. *J. Org. Chem.* **1999**, *64*, 5661. (d) Kumpf, R. A.; Dougherty, D. A. *Science* **1993**, *261*, 1708.
11. Cui, C.; Kim, K. S. *J. Phys. Chem. A* **1999**, *103*, 2751.
12. Michaux, G.; Reisse, J. *J. Am. Chem. Soc.* **1982**, *104*, 6895.
13. Valleau, J. P.; Torrie, G. M. *Statistical Mechanics, Part A*; Berne, B. J., Ed.; Plenum: New York, 1977; p 169.
14. Jorgensen, W. L. *J. Phys. Chem.* **1983**, *87*, 5304.
15. Rebertus, D. W.; Berne, B. J.; Chandler, D. *J. Chem. Phys.* **1979**, *70*, 3395.
16. Mezei, M.; Mehrotra, P. K.; Beveridge, D. L. *J. Am. Chem. Soc.* **1985**, *107*, 2239.
17. Chandrasekhar, J.; Jorgensen, W. L. *J. Am. Chem. Soc.* **1985**, *107*, 2974.
18. Postma, J. P. M.; Berendsen, H. J. C.; Haak, J. R. *Faraday Symp. Chem. Soc.* **1982**, *17*, 55.
19. Tembe, B. L.; McCammon, J. A. *Comput. Chem.* **1984**, *8*, 281.
20. Kollman, P. A. *Chem. Rev.* **1993**, *93*, 2395.
21. Leo, A.; Hansch, C.; Elkins, D. *Chem. Rev.* **1971**, *71*, 525.
22. Hansch, C.; Leo, A. *Substituent Constants for Correlation Analysis in Chemistry and Biology*; Wiley: New York, 1979.
23. Dunn, W. J.; Block, J. S.; Pearlman, R. S. *Partition Coefficient; Determination and Estimation*; Pergamon: New York, 1986.
24. Dunn, W. J.; Koehler, M. G.; Grigoras, S. *J. Med. Chem.* **1987**, *30*, 1121.
25. Klopman, G.; Namboodiri, K.; Schochet, M. *J. Comput. Chem.* **1985**, *6*, 28.
26. Jorgensen, W. L. *BOSS Version 3.8*; Yale University: New Haven, CT, 1997.
27. Jorgensen, W. L.; Ravimohan, C. *J. Chem. Phys.* **1985**, *83*, 3050.
28. (a) Jorgensen, W. L.; Briggs, J. M. *J. Am. Chem. Soc.* **1989**, *111*, 4120. (b) Kim, H-S. *Chem. Phys. Lett.* **2000**, *317*, 553. (c) Kim, H-S. *Chem. Phys.* **2000**, *253*, 305.
29. Zwanzig, R. W. *J. Chem. Phys.* **1954**, *22*, 1420.
30. (a) Jorgensen, W. L. *Acc. Chem. Res.* **1989**, *22*, 184. (b) Essex, J. W.; Reynolds, C. A.; Richards, W. G. *J. Chem. Soc. Chem. Commun.* **1989**, *11*, 62.
31. Cieplak, P.; Kollman, P. A. *J. Am. Chem. Soc.* **1988**, *110*, 3714.
32. Jorgensen, W. L.; Blake, J. F.; Buckner, J. K. *Chem. Phys.* **1989**, *129*, 193.
33. Jorgensen, W. L. *J. Phys. Chem.* **1986**, *90*, 6379.
34. Jorgensen, W. L.; Tirado-Rives, J. *Am. Chem. Soc.* **1988**, *110*, 1657.
35. Christian R. *Solvents and Solvent Effects in Organic Chemistry*, 2nd ed.; VCH: 1988; p 20.
36. Abraham, R. J.; Bretschneider, E. *Internal Rotation in Molecules*; Orville-Thomas, W. J., Ed.; Wiley: London, 1974; Chapter 13.
37. Jorgensen, W. L.; Briggs, J. M.; Leonor, C. M. *J. Phys. Chem.* **1990**, *94*, 1683.
38. Åqvist, J. *J. Phys. Chem.* **1990**, *94*, 8021.
39. Florian, J.; Warshel, A. *J. Phys. Chem. B* **1999**, *103*, 10282.
40. Babu, C. S.; Lim, C. *J. Phys. Chem. B* **1999**, *103*, 7958.
41. Migliore, M.; Fornili, S. L.; Spohr, E.; Palinkas, G. K.; Heizinger, Z. *Naturforsh* **1985**, *41a*, 828.
42. Lee, S. H.; Rasaiah, J. C. *J. Phys. Chem.* **1996**, *100*, 1420.
43. Lybrand, T. P.; Kollman, P. A. *J. Chem. Phys.* **1985**, *83*, 2923.
44. Lee, H. M.; Kim, J.; Lee, S.; Mhin, B. J.; Kim, K. S. *J. Chem. Phys.* **1999**, *111*, 3995.
45. Chang, T-M.; Dang, L. X. *J. Phys. Chem. B* **1999**, *103*, 4714.
46. Rao, M.; Berne, B. J. *J. Phys. Chem.* **1981**, *85*, 1498.
47. (a) Bockris, J. O'M.; Reddy, A. K. N. *Modern Electrochemistry*; Prenum Press: New York, 1970; Vol. 1, Chapter 2, p 45. (b) Chung, J. J.; Kim, H-S. *Bull. Korean Chem. Soc.* **1993**, *14*, 220. (c) Desnoyers, J. E.; Jolicoeur, C. *Modern Aspects of Electrochemistry*; Bockris, J. O'M., Conway, B. E., Eds.; Plenum Press: New York, 1969; Vol. 5, p 1.
48. (a) Neilson, G. W.; Enderby, J. E. *Annu. Rep. Progr. Chem., Sect. C* **1979**, *76*, 185. (b) Enderby, J. E.; Neilson, G. W. *Rep. Progr. Phys.* **1981**, *44*, 38. (c) *Water: A Comprehensive Treatise*; Franks, F., Ed.; Plenum Press: New York, 1979; Vol. 6, Chapter 1.
49. Mezei, M.; Beveridge, D. L. *J. Chem. Phys.* **1981**, *74*, 6902.